Journal of Organometallic Chemistry, 296 (1985) 209–228
Elsevier Sequoia S.A., Lausanne – Printed in The Netherlands

REVERSIBLE SYNTHESES OF MONO-(CYCLOPENTADIENYL)RHODIUM-TRI-RUTHENIUM CLUSTER COMPLEXES AND $(\eta\text{-}C_5Me_5)_2Rh_2Ru_2(CO)_7$; CRYSTAL AND MOLECULAR STRUCTURES OF $CpRhRu_3\{\mu\text{-}H\}_2\{\mu\text{-}CO\}(CO)_9$, $Cp = \eta\text{-}C_5H_5$ OR $\eta\text{-}C_5Me_5$ AND $(\eta\text{-}C_5Me_5)Rh\{\mu\text{-}H\}_2Ru_3\{\mu\text{-}H\}_2(CO)_9$ *

W. EDWARD LINDSELL*

Department of Chemistry, Heriot-Watt University, Edinburgh EH14 4AS, U.K. (Great Britain)

CAROLYN B. KNOBLER and HERBERT D. KAESZ *

Department of Chemistry and Biochemistry, University of California, Los Angeles, California, 90024 (U.S.A.)

(Received April 19th, 1985)

Summary

The mixed metal complexes $CpRhRu_3\{\mu\text{-}H\}_2\{\mu\text{-}CO\}(CO)_9$, (**3a**: $Cp = \eta\text{-}C_5H_5$; **3b**: $Cp = \eta\text{-}C_5Me_5$) **4b**: $(\eta\text{-}C_5Me_5)RhRu_3\{\mu\text{-}H\}_4(CO)_9$, **5**: $(\eta\text{-}C_5Me_5)_2Rh_2Ru_2(CO)_7$) are formed when H_2 is bubbled through solutions of $Ru_3(CO)_{12}$ and the respective $CpRh(CO)_2$ at 70–90°C. These are easily disrupted at 25°C back into the starting materials under an atmosphere of CO.

Using ^{13}CO, the starting materials are obtained with complete ^{13}CO exchange. While $CpRh(CO)_2$ undergoes exchange at 25°C with ^{13}CO at atmospheric pressure, $Ru_3(CO)_{12}$ does not, nor does it exchange in the presence of simply an added amount of $CpRh(CO)_2$. Attachment of the CpRh moiety to the Ru_3 skeleton as in the products obtained in this work thus leads, under ^{13}CO, to the completely enriched starting materials $Ru_3(^{13}CO)_{12}$ and $CpRh(^{13}CO)_2$.

Structures of three new products have been determined using a Picker (FACS-1) four circle automated diffractometer and graphite-monochromatized Mo-K_α radiation. For **3a**, 3831 unique reflections with $I > 3\sigma(I)$ were used in the refinement; final discrepancy indices, $R = 0.030$ and $R_w = 0.050$. Complex **3a** crystallizes in the monoclinic space group $P2_1/n$; cell dimensions a 8.1856(5), b 15.0706(10), c 16.3013(12) Å, and β 91.033(1)°; calculated density 2.49 g cm^{-3}. For **3b**, 4801 unique reflections with $I > 3\sigma(I)$ were used in the refinement; final discrepancy indices, $R = 0.026$ and $R_w = 0.042$. Complex **3b** crystallizes in the monoclinic space group $P2_1/n$ in a cell having the dimensions of a 8.7580(5), b 14.5578(8), c

---

* Dedicated to Professor Lamberto Malatesta in recognition of his important contributions to the chemistry of the transition metals in their low oxidation states.

0022-328X/85/$03.30

19.829(1) Å, and β 97.591(2)°; calculated density 2.18 g cm^{-3}. For **4b**, 6756 unique reflections with $I > 3\sigma(I)$ were used in the refinement; final discrepancy indices, $R = 0.030$ and $R_w = 0.040$. Complex **4b** crystallizes in the monoclinic space group $P2_1/a$; cell dimensions a 17.470(1), b 18.451(1), c 17.200(1) Å, and β 114.684(1)°; calculated density 2.10 g cm^{-3}.

Metal atoms in all three structures were located by direct methods (MULTAN80). All other nonhydrogen atoms were then located by difference maps. Hydrogen atoms bridging various edges of the clusters were located after all hydrogen atoms in the η-C_5H_5 (= Cp) or η-$C_5(CH_3)_5$ (= Cp*) groups were refined isotropically in calculated positions. Each of the crystals studied consists of discrete molecules of the complexes, each with a triangle of ruthenium atoms capped by a CpRh or Cp*Rh group. Isomeric structures are observed for **3a** and **3b**. In the former, a CO group is found bridging between one Ru atom and the Rh atom while one each of two cluster-bound hydrogen atoms bridge two separate edges of the Ru_3 triangle. In **3b**, both a CO group and one of the cluster-bound hydrogen atoms are found bridging between Rh and two separate Ru atoms of the Ru_3 triangle. The remaining cluster-bonded hydrogen atom is found bridging one edge of the Ru_3 triangle. In **4b**, two of the cluster-bound hydrogen atoms are found (one each) on two edges of the Ru_3 triangle. The other two are found bridging each of two of the Ru–Rh bonds. The metal–metal separations in the three structures are summarized as follows. Unbridged Ru–Ru and Rh–Ru fall in the ranges 2.765(1) to 2.813(1) Å and 2.707(1) to 2.752(1) Å, respectively; the Rh–μ-(CO)–Ru separations are 2.727(1) (in **3a**) and 2.7515(1) (in **3b**). Ru–μ-(H)–Ru separations fall in the range 2.870(1) to 2.938(1) Å while Rh–μ-(H)–Ru fall in the range 2.871(1) to 2.9169(1) Å.

Introduction

We wished to introduce the CpRh moiety into cluster complexes of ruthenium in order to make use of the nuclear spin of ^{103}Rh in elucidating intramolecular exchange processes. Prior to this work, only two Ru/Rh mixed metal cluster complexes were known, namely, $[Ru_3Rh_2(CO)_{13}(PEt_3)(\mu_4\text{-}PPh)]$ [1], and $[Ru_2Rh_2\{\mu\text{-}H\}_2(CO)_{12}]$ [2]. Mixed metal complexes of the congeners of these two metals were also known [3,4], which are mentioned in the relevant portions of the next section. A preliminary account of the present work has been submitted [5].

Results

Syntheses of the mixed metal cluster complexes and their reversion to the starting materials under surprisingly mild conditions in a CO atmosphere are summarized in Scheme 1. Spectroscopic properties for the new complexes are presented in Table 1.

The isomeric structures indicated for **3a** and **3b** in Scheme 1 anticipate the results of the structure determinations (see below). This parallels isomerism observed in the Co/Os or Rh/Os homologues of **3a** or **3b**, $(\eta\text{-}C_5H_5)M(\mu\text{-}CO)Os_3(\mu\text{-}H)_2(CO)_9$ (M = Co (**6a**) [3a,b]; M = Rh (**7**) [3c]), and $(\eta\text{-}C_5Me_4Et)Co(\mu\text{-}CO,\mu\text{-}H)Os_3(\mu\text{-}H)(CO)_9$ (**6b**) [4]. In addition, for **3b** we find a single bridging CO absorption in the solid (KBr pellet, see Table 1), while in solution three bridging CO absorptions are

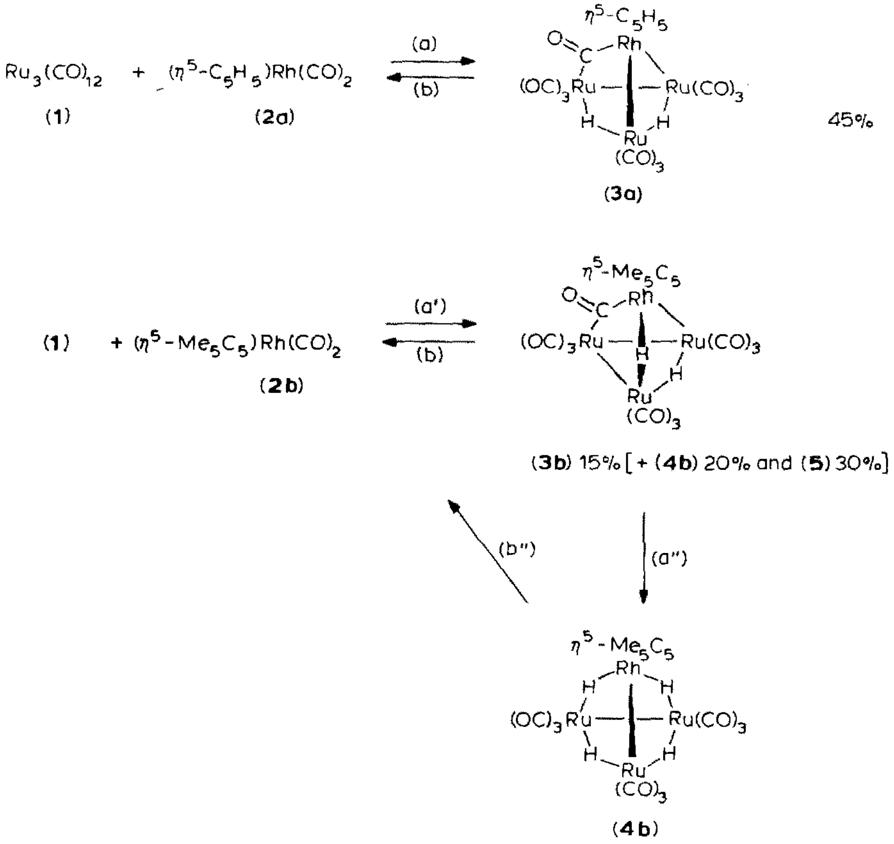

(**5**): $(\eta^5\text{-}Me_5C_5)_2Rh_2Ru_2(CO)_7$
(a): H_2, 1 atm/octane/90°C/2 h
(a'): H_2, 1 atm/heptane/70° C/1.25 h
(a"): H_2, 1 atm/octane/22° C/4 d (100% conv.)
(b): CO, 1 atm/25° C/$t_{1/2}$ ca. 2 h
(b"): CO, 1 atm/25° C/$t_{1/2}$ ca. 4 h

SCHEME 1

TABLE 1

SPECTROSCOPIC DATA

	IR: ν(CO) (cm^{-1})
3a	[a] 2088(m), 2066(s), 2049(s), 2018(m), 2009(m), 2001(w), 1982(w), 1827(m)
3b	[b] 2072(m), 2041(s), 2012(vs), 2000(m), 1983(s), 1960(w), 1934(w), 1790(s)
	[c,d] 2089(m), 2080(m), 2060(s), 2051(m), 2042(vs), 2035(m), 2013(m), 2004(w), 1994(w), 1831(w), 1812(w), 1800(w)
4b	[a] 2079(s), 2051(vs), 2043(vs), 2008(s), 2001(w), 1994(w), 1989(m)
5	[a] 2042(s), 2015(vs), 1982(m), 1974(m), 1959(w), 1709(w), 1684(w)
	^{1}H NMR δ(ppm), (J (Hz)) [e]
3a	5.16 (s, C_5H_5); −17.2 (s) $(\mu\text{-}H)_2$
3b	1.63 (s), 1.54 (s) $(C_5(CH_3)_5)$; −13.0 (s), −17.0 (d, J 8), −20.3 (s) (μ-H) [d]
4b	1.71 (s, $(CH_3)_5C_5$); −15.93 (d, J 13.5), $(\mu\text{-}H)_4$
5	1.64 (s, $(CH_3)_5C_5$)

[a] Hexane solution. [b] KBr. [c] Light petroleum solution, b.p. 40–60°C. [d] For an equilibrium mixture of apparently three isomers, see text. [e] 90 MHz, 26°C, $C_6D_5CD_3$ sol'n; s, singlet; d, doublet.

seen, accompanied by a more complex terminal CO absorption pattern. Despite a single isomer in the solid, several isomers exist in solution. This also parallels observations on its Co/Os_3 homologue, **6b** [4]; a Co/Os_3 analogue of **4b**, namely (η-C_5Me_4Et)$CoOs_3(\mu$-$H)_4(CO)_9$ (**8**), has also been reported [4].

Finally, we should take note of the apparent count of 58 e^- in complex **5**, assuming only 2 e^- donated by each CO group. This is coupled with observation of two absorptions in the bridging carbonyl region (Table 1). These observations indicate the presence of two bridging groups as observed in CpCo(CO)(μ-η^1,η^2-CO)Zr(η-$Me_5C_5)_2$, ν(CO) 1737 and 1683 cm^{-1}, [6a] and related derivatives [6b], leading us to propose one of the two structures **a** or **b** for complex **5**. A (μ-η^1,η^2-CO) group (ν(CO) 1645 cm^{-1}) was first observed in the complex $(dpm)_2Mn_2(CO)_5$, dpm = bis(diphenylphosphino)methane [6c,d], similarly exhibiting an apparent deficiency of two in its electron count.

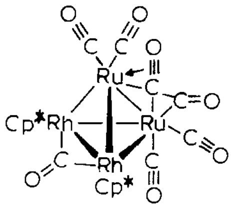

(a)

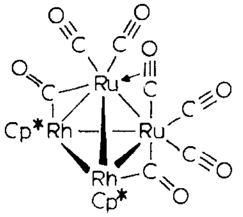

(b)

Reactions with CO. We discovered that **3a, 3b**, or **4b** are easily disrupted back into starting materials in attempts to enrich them with ^{13}CO. The conversions occur with complete ^{13}CO exchange giving products that are characterized by their carbonyl region absorptions (all in hexane) (cm^{-1}): $Ru_3(^{13}CO)_{12}$, 2011vs, 1985s, and 1966m, cf. 2061vs, 2031s and 2011m for $Ru_3(CO)_{12}$; $CpRh(^{13}CO)_2$, 2000s, 1985w, 1939s and 1908w, cf. 2048s, 2033w, 1985s, 1955w for $CpRh(CO)_2$, and, $Cp^*Rh(^{13}CO)_2$, 1978s, 1962w, 1917s and 1880w, cf. 2025s, 2009w, 1963s, 1933w for $Cp^*Rh(CO)_2$.

While $CpRh(CO)_2$ undergoes exchange at 25°C with ^{13}CO at atmospheric pressure, $Ru_3(CO)_{12}$ does not, nor does it exchange in the presence of an added amount of $CpRh(CO)_2$. Thus, attachment of the CpRh moiety to the Ru_3 skeleton as in **3a**, **3b**, or **4b**, is required to obtain completely enriched products under ^{13}CO. Presumably the exchange occurs at the Rh atom in the starting material or some Rh/Ru_3 intermediate cluster and is equilibrated over the entire ensemble of CO groups before cleavage of the CpRh group from the tetrametal cluster. Absorptions not belonging to the starting materials nor to the final products are seen at intermediate stages of the exchange but the products to which they may belong have not been pursued in this work. The reaction of **5** with CO is to be investigated shortly which results we hope to add in proof (see p. 228).

The ready dissociation of these products under CO is reminiscent of like observations on mixed metal clusters of Fe/Ru_2/Os, Fe/Ru_3 or Co/Ru_3 [7]. By comparison, we find that the mixed metal cluster $Rh_2Ru_2\{\mu$-$H\}_2(CO)_{12}$ (**9**) [2] is completely disrupted into intermediate complexes within a period of 17 h under an atmosphere of CO at 25°C ($t_{1/2}$ ca. 4 h). An additional 73 h are required to convert the intermediates into $Rh_4(CO)_{12}$ and a mixture of $Ru_3(CO)_{12}$ and $Ru(CO)_5$. Disruptions of (η-C_5Me_4Et)$Co(\mu$-$CO)Os_3(\mu$-$H)_2(CO)_9$ (**6b**) or (η-C_5Me_4Et)$CoOs_3$(μ-

$H)_4(CO)_9$ (**8**) are reported to require 50 bar of CO and temperatures of 50 or 150°C and 2 or 4 h, respectively [4]. The ease of the cluster disruptions observed in the present work should be taken into account in postulating or attempting catalysis by these mixed metal species under homogeneous conditions [2,8].

To elucidate the isomerism for complexes **3a** and **3b** and to characterize the tetrahydrido complex **4b**, structure studies were undertaken which are described in the sections which follow.

Experimental

General. Solvents and reagents were of commercial reagent grade and were dried and redistilled under nitrogen. The petroleum ether cited throughout this section is that from Mallinckrodt ("AR", b.p. 35–60°C). Starting materials: $Ru_3(CO)_{12}$ (**1**) was prepared from $RuCl_3 \cdot 3H_2O$ [9a,b]; $(\eta\text{-}C_5H_5)Rh(CO)_2$ (**2a**) was prepared from $[Rh(CO)_2Cl]_2$ and $Na(C_5H_5)$ [9c]. $(\eta\text{-}Me_5C_5)Rh(CO)_2$ (**2b**) was purchased from Strem Chemicals. $Rh_2Ru_2(\mu\text{-}H)_2(CO)_{12}$ (**9**) was synthesized according to the literature report [2].

Although the products in this work are generally air stable, reactions, filtrations and recrystallizations were routinely carried out under a purified nitrogen atmosphere using Schlenk techniques. Chromatographic separations and handling of neutral complexes can be done in air if exposure is limited to a few hours. Carbonyl infrared spectra were recorded on a Nicolet MX-1 FT-IR spectrometer. ^1H and ^{31}P NMR spectra were recorded on a Bruker WP-200 and a JEOL FX90Q spectrometers; ^1H NMR were calibrated against internal residual $CHCl_3$ at δ 7.25 ppm. Fast atom bombardment mass spectra (FAB-MS) were obtained using a locally constructed FAB gun mounted on a modified AEI MS-9 double focusing mass spectrometer. A 6 keV xenon atom beam was used with gun tube current at 1 mA. A mg of compound is slurried into 1 μl of a liquid matrix composed of 9 parts of 18-crown-6 ether (Aldrich) to 1 part tetraglyme. A trace (0.2 μl) of Santovac-5 oil (Monsanto) is added before insertion into the mass spectrometer. Elemental analyses were performed by Schwarzkopf Laboratories, Inc.

Preparation of $(\eta\text{-}C_5H_5)Rh\{\mu\text{-}(CO\}Ru_3\{\mu\text{-}H\}_2(CO)_9$ *(3a)*

A steady stream of dihydrogen is bubbled through a solution of $Ru_3(CO)_{12}$ (**1**, 400 mg; 0.63 mmol) and excess $CpRh(CO)_2$ (**2a**, 200 mg; 0.89 mmol) in octane (80 ml) at 90°C for 2 h. The initially yellow/orange solution turns dark brown during this period. After cooling to ambient temperature, the solution is reduced in volume to ca. 30 ml and the contents chromatographed on a column of silica gel (60–200 mesh). With petroleum ether, a yellow band elutes first which consists of $Ru_4(\mu\text{-}H)_4(CO)_{12}$ [10a] admixed with unreacted **1** (ca. 110 mg). This is followed by a second dark brown band which, on evaporation, yields **3a** (180–250 mg; 38–53%). With dichloromethane, a deep red band is eluted giving $Cp_2Rh_2(CO)_3$ (ca. 20 mg) [10b,c].

Elemental analysis. Found: C, 22.83; H, 1.45. $RhRu_3C_{15}H_7O_{10}$ (**3a**) calcd.: C, 23.91; H, 0.94%.

Preparation of $(Cp^\star)Rh\{\mu\text{-}CO,\mu\text{-}H\}Ru_3\{\mu\text{-}H\}(CO)_9$ *(3b),* $(Cp^\star)Rh\{\mu\text{-}H\}_2Ru_3\{\mu\text{-}H)_2(CO)_9$ *(4b), and* $(Cp^\star)_2Rh_2Ru_2(CO)_7$ *(5),* $Cp^\star = \eta\text{-}Me_5C_5$

A steady stream of dihydrogen is passed through a solution of **1** (200 mg; 0.31

TABLE 2

CRYSTAL DATA FOR (η-Cp)RhRu$_3$(μ-H)$_2$(CO)$_9$(μ-CO), (**3a**: Cp = C_5H_5; **3b**: Cp = C_5Me_5) AND (η-C_5Me_5)Rh(μ-H)$_2$Ru$_3$(μ-H)$_2$(CO)$_9$ (**4b**)

Compound	**3a**	**3b**	**4b**
Formula	$RhRu_3C_{15}H_7O_{10}$	$RhRu_3C_{20}H_{17}O_{10}$	$RhRu_3C_{19}H_{19}O_9$
Formula wt.	753.33	823.46	797.5
a (Å)	8.1856(5)	8.7580(5)	17.470(1)
b (Å)	15.0706(10)	14.5578(8)	18.451(1)
c (Å)	16.3013(12)	19.829(1)	17.200(1)
β (deg)	91.033(1)	97.591(2)	114.684(1)
V (Å^3)	2003.47	2497.23	5037.6(5)
Z	4	4	8
ρ(calc) (g cm^{-3})	2.49	2.18	2.10
Crystal system	Monoclinic [a]	Monoclinic [a]	Monoclinic [a]
Space group	$P2_1/n$	$P2_1/n$	$P2_1/a$
Crystal size (approx.) (mm)	0.405 × 0.20 × 0.175	0.16 × 0.16 × 0.37	0.2 × 0.14 × 0.45
Boundary faces	$011\ 01\bar{1}\ 0\bar{1}\bar{1}\ 0\bar{1}1\ \bar{1}00\ 100\ \bar{2}10$ [b]	$011\ 0\bar{1}1\ 0\bar{1}\bar{1}\ 01\bar{1}\ \bar{2}\bar{1}2\ 2\bar{1}2$ [b]	$00\bar{1}\ 20\bar{1}\ 001\ \bar{2}01\ \bar{1}\bar{2}1\ 12\bar{1}$ [c]
Temperature (K)	298	298	295
Abs. coeff. (μ) (cm^{-1}) [e]	30.135	24.273	24.09
Transmission factors (F^2)	0.5676–0.6120	0.6444–0.7349	0.6184–0.7488
$\theta - 2\theta$ Scan rate (deg min^{-1})	6.0	4.5	6
Scan width [f]	−1.3 to +1.4	−1.3 to +1.4	−1.4 to +1.4
2θ limits (deg)	0–54	0–54	0–50
Reflections collected	4388	5470	8853
No. of unique data ($I_0 > 3\sigma I_0$)	3831	4801	6756
Total no. of variables [g]	270	315	551
R [h]	0.030	0.026	0.030
R_w [i]	0.050	0.042	0.040
GOF [j]	1.942	1.654	1.342

---

[a] Observations $+h$, $+k$, $\pm l$. [b,c,d] At distances from a common point, respectively (mm): (b) 0.19 0.0 0.0 0.18 0.0 0.405 0.03; (c) 0.16 0.0 0.0 0.16 0.0 0.37; (d) 0.0 0.0 0.2 0.14 0.0 0.45. [e] Radiation: Mo-K_α 0.7107 Å. [f] deg below Mo-$K_{\alpha 1}$ to deg above Mo-$K_{\alpha 2}$. [g] In the last refinement. [h] $R = \Sigma(||F_0| - |F_c||)/\Sigma|F_0|$. [i] $R_w = [\Sigma w(|F_0| - |F_c|)^2/\Sigma w|F_0|^2]^{1/2}$; $w = 1/(\sigma^2|F_0|)$. [j] Error in observation of unit wt. $= [\Sigma w(|F_0| - |F_c|)^2/(N_0 - N_v)]^{1/2}$.

mmol) and $Cp^{\star}Rh(CO)_2$ (**2b**, 92 mg; 0.31 mmol) in heptane (75 ml) at 70°C for 1.25 h. The solution turns dark brown during this time. After cooling to ambient temperature, chromatography of the reaction mixture on silica gel (60–200 mesh) yields the following. With petroleum ether, a broad yellow band consisting of $Ru_4\{\mu\text{-}H\}_4(CO)_{12}$ is eluted first accompanied by **1** and a little **2b** (< 40 mg). Continuing with petroleum ether, a deep red band is next eluted which consists of **4b**; yield, 50 mg (20%) upon evaporation. This material can be recrystallised from hexane at −30°C to give large brown crystals. With a mixture of petroleum ether/dichloromethane (10/1), a deep red-brown band is eluted which upon evaporation affords **3b** (39 mg; 15%). This can be recrystallised from hexane/dichloromethane at −30°C to give brown parallelepipeds. Continuing with a 5/1 mixture of petroleum ether/dichloromethane, a second deep red-brown band is eluted giving a brown product, which can be recrystallised from hexane/dichloromethane at −30°C to give brown needle-like prisms of **5** (40 mg, 30% yield). FAB-MS confirms the formula weight.

Elemental analyses. Found: C, 29.35; H, 2.12. $RhRu_3C_{20}H_{17}O_{10}$ (**3b**) calcd.: C, 29.17; H, 2.08%. Found: C, 28.52; H, 2.35. $RhRu_3C_{19}H_{19}O_9$ (**4b**) calcd.: C, 28.62; H, 2.40%. Found: C, 37.00; H, 3.05%. $Rh_2Ru_2C_{27}H_{30}O_7$ (**5**) calcd.: C, 37.08; H, 3.46%.

Conversion of **3b** (30 mg in 30 ml octane) to **4b** is achieved under an atmosphere of H_2 at 22°C. Yield: spectroscopically quantitative in 4.5 days.

Reactions with CO

(i) Either **3a** (10 mg) or **3b** (6 mg) are stirred in 6 ml of hexane under CO (20 cm^3, 1 atm) at 22°C. IR spectra showed total conversion to **1** and **2a** or **2b** within 4.5 h. To rule out that these reactions are not brought about by the background illumination, they were also carried out in the dark with similar results.

Using 60 cm^3 of 99.9% ^{13}CO in (i), completely exchanged products are obtained. Under the same conditions and in the dark, **1** does not show any exchange with ^{13}CO, after 18 h. Unprotected from the background illumination of laboratory fluorescent lights, approximately 30% exchange is observed after 4 days.

(ii) With **4b**, 15 mg in 3 ml hexane are stirred under an atmosphere of CO as in (i). Conversion to **1** and **2b** is essentially complete in 7.5 h. At no stage is there any evidence for any intermediates.

(iii) $Rh_2Ru_2(\mu\text{-}H)_2(CO)_{12}$ (**9**, 10 mg in 5 ml hexane) is treated with CO as in (i). Complete disappearance of starting material requires 17 h. At this point the IR spectrum shows the presence of $Rh_4(CO)_{12}$ (e.g. 1885 cm^{-1}, μ-CO), $Ru(CO)_5$ (2035, 1999 cm^{-1}) and other unidentified species. The latter as well as $Ru(CO)_5$ convert to **1** over an additional 3 d of stirring.

Crystallographic study

Data collection

Air and X-ray stable single crystals were obtained for each of the three compounds whose structures were determined. Data for each of the crystals and parameters related to data collection and refinement are given in Table 2. Crystals were grown at ambient temperature by slow evaporation: for **3a** or **3b**, from CH_2Cl_2/hexane solutions, dark brown trapezoidal crystals or dark brown parallelepiped crystals (respectively) are obtained; for **4b**, from hexane at −30°C, brown prisms. The crystals were each glued to the tip of a glass fiber and mounted on a goniometer head of a Picker (FACS-1) four-circle automated diffractometer modified at U.C.L.A. by C.E. Strouse for operation under control of a VAX 11/750 computer. For **3a** and **3b** the faces $(0, k, l)$, k and $l = 1$ were roughly parallel to the ϕ axis of the instrument; for **3a**, the crystal selected for study had one vertex truncated by the plane face $(\bar{2}, 1, 0)$. For **4b** the crystal was mounted with faces $(0, 0, \bar{1}; 2, 0, \bar{1}; 0, 0, 1$ and $\bar{2}, 0, 1)$ roughly parallel to the fiber axis.

Lattice parameters and standard errors were determined by least squares refinement of the angular settings of a number of Mo-K_α peaks centered on the diffractometer: for **3a**, 25 peaks in the range $11° < 2\theta < 21°$; for **3b**, 45 peaks in the range $10° < 2\theta < 21°$; for **4b**, 45 peaks in the range $12° < 2\theta < 21°$. The refined unit cell parameters and other specifics relevant to the data collection are given in Table 2. For **4b**, there are two independent molecules in the unit cell (cf. Table 2); these are designated as **4b** and **4b′** when molecular parameters are cited.

Background for each peak was determined from the peak profile. The intensities of three standard reflections were recorded after every 97 intensity measurements to monitor crystal and diffractometer stability; standard reflections, respectively, for **3a**, $(3, 5, 0)$, $(2, 0, \bar{4})$, $(1, 1, 5)$; for **3b**, $(1, 0, 7)$, $(0, 5, 1)$, $(3, \bar{4}, 1)$; for **4b**, $(4, 3, \bar{5})$, $(5, 5, \bar{1})$, $(4, 2, 4)$. The variations in the standards were random for all three samples, all showing deviations from the respective mean values of less than 2%.

A survey of the complete data set for each structure showed systematic absences consistent with assignment of the space group shown in Table 2: for **3a** and **3b**, reflections $(h, 0, l)$ $h + l \neq 2n$, and $(0, k, 0)$ $k \neq 2n$; for **4b**, reflections $(h, 0, l)$ $h \neq 2n$, and $(0, k, 0)$ $k \neq 2n$. The total number of independent reflections measured for each compound and range of 2θ are given in Table 2, as well as the number of reflections used in the solution and refinement of each structure. All of the latter reflections were corrected for Lorentz and polarization effects and converted to $|F_0|$ and $\sigma(|F_0|)$ by means of the CARESS program (see next paragraph for description of computer programs).

Solution and refinement of the structures

All calculations were performed on a VAX 11/750 computer (Chemistry Department of UCLA). Programs used for the structure determination consist in all cases of local modifications edited by Dr.C.E. Strouse and his research group: for data reduction, CARESS, originally written by R.W. Broach (Univ. of Wisconsin) and P. Coppens, P. Becker and R.H. Blessing (SUNY, Buffalo NY); for Fourier analysis, adaptations of MULTAN80, P. Main (Univ. of York, UK); for full matrix least-squares and error analysis, ORFLS and ORFFE, W.R. Busing, K.O. Martin and H.A. Levy (Oak Ridge National Lab., TN); for absorption correction, ABSN, P. Coppens; for least-squares planes, MG84, P. Gantzel and K.N. Trueblood; for thermal ellipsoid plot program, ORTEP II, C.K. Johnson (Oak Ridge Nat. Lab.); for structure factor table listing, PUBLIST, E. Hoel.

Scattering factors for neutral rhodium, ruthenium, oxygen and carbon atoms were taken from Table 2.2A of ref. 11a while those for hydrogen were from Stewart et al. [11b]. Both real ($\Delta f'$) and imaginary ($\Delta f''$) components of anomalous dispersion were included for rhodium and ruthenium using the values in Table 2.3.1 of ref. 11a. The function minimized during least-squares refinement and the discrepancy indices are given in Table 2.

Reasonable positions for all the metals atoms in each of the three structures were obtained by direct methods (MULTAN80). Full-matrix least-squares refinement on the metal atoms with isotropic temperature factors followed by difference Fourier synthesis in each case revealed the positions of other atoms and, after further refinement, the positions of all non-hydrogen atoms. Refinement with isotropic temperature factors for all non-hydrogen atoms produced the following residuals: for **3a**, $R = 0.068$ and $R_w = 0.104$; for **3b**, $R = 0.062$ and $R_w = 0.097$, and for **4b**, $R = 0.077$ and $R_w = 0.103$. The data were then corrected for the effects of absorption, see data presented in Table 2. Least-squares refinement with anisotropic thermal parameters for all the metal atoms gave the following residuals: for **3a**, $R = 0.049$ and $R_w = 0.076$; for **3b**, $R = 0.030$ and $R_w = 0.053$, and for **4b**, $R = 0.048$ and $R_w = 0.067$. For **3a** (and **3b**) three cycles of further refinement with anisotropic thermal parameters for all non-hydrogen atoms afforded the R factors shown in Table 2.

At this stage it was possible to locate hydrogen atoms as follows. For **3a**, the

TABLE 3A

POSITIONAL PARAMETERS OF (η^5-C_5H_5)Rh(μ-CO)Ru_3(μ-H)$_2$(CO)$_9$ (3a)

Atom	*x/a*	*y/b*	*z/c*
Rh	0.70588(5)	0.31652(3)	0.36063(2)
Ru(01)	0.51996(5)	0.17976(2)	0.30222(2)
Ru(02)	0.76586(5)	0.15687(3)	0.43400(2)
Ru(03)	0.48231(5)	0.25000(3)	0.46443(2)
O(b)	0.9906(5)	0.2250(3)	0.2933(3)
O(11)	0.2941(6)	0.0270(3)	0.2532(3)
O(12)	0.3069(6)	0.3200(3)	0.2196(3)
O(13)	0.7388(6)	0.1555(3)	0.1554(3)
O(21)	0.6134(6)	0.0412(3)	0.5655(3)
O(22)	1.0255(6)	0.0188(4)	0.3941(4)
O(23)	0.9722(6)	0.2568(4)	0.5581(3)
O(31)	0.2710(7)	0.1352(4)	0.5722(4)
O(32)	0.6400(7)	0.3548(4)	0.6038(3)
O(33)	0.2239(6)	0.3903(4)	0.4341(3)
C(b)	0.8774(6)	0.2347(4)	0.3338(3)
C(11)	0.3794(6)	0.0824(4)	0.2730(3)
C(12)	0.3886(7)	0.2685(4)	0.2498(3)
C(13)	0.6571(7)	0.1655(3)	0.2100(3)
C(21)	0.6587(7)	0.0878(4)	0.5151(3)
C(22)	0.9298(7)	0.0688(4)	0.4080(4)
C(23)	0.8950(7)	0.2183(5)	0.5129(4)
C(31)	0.3488(8)	0.1781(4)	0.5332(4)
C(32)	0.5840(8)	0.3159(4)	0.5519(4)
C(33)	0.3191(8)	0.3372(4)	0.4446(4)
C(41)	0.8237(11)	0.4451(5)	0.4004(7)
C(42)	0.6590(10)	0.4558(4)	0.4041(5)
C(43)	0.5923(9)	0.4436(4)	0.3257(6)
C(44)	0.7280(16)	0.4279(5)	0.2725(4)
C(45)	0.8669(11)	0.4271(5)	0.3232(8)
H(12)	0.6300(65)	0.1007(39)	0.3521(34)
H(13)	0.3862(97)	0.1769(47)	0.3787(44)

hydrogen atoms of the cyclopentadienyl ring were fixed in calculated positions with C–H 1.00 Å giving $R = 0.031$ and $R_w = 0.051$ on least-squares refinement. A difference Fourier synthesis clearly revealed the metal bound hydrogen atoms and final least-squares refinement including the positions of the metal hydrogen atoms produced the final discrepancy indices given in Table 2.

For **3b**, at least one hydrogen atom of each of the cyclopentadienyl-attached methyl groups was located and, using these positions, the fifteen methyl-hydrogen atoms were fixed in calculated positions with C–H 1.00 Å and H–C–H 109.5°; least-squares refinement gave residuals of $R = 0.027$, $R_w = 0.044$. A difference Fourier synthesis clearly revealed the metal bound hydrogens at this stage and further least-squares refinement, including these metal-hydrogen atoms, produced final discrepancy indices shown in Table 2.

TABLE 3B

POSITIONAL PARAMETERS OF (η^5-Me_5C_5)Rh(μ-CO,μ-H)Ru_3(μ-H)$(CO)_9$ (**3b**)

Atom	*x*	*y*	*z*
Rh	0.44541(3)	0.26424(2)	0.18740(1)
Ru(O1)	0.53922(4)	0.22358(2)	0.05478(2)
Ru(O2)	0.24754(3)	0.17684(2)	0.08846(1)
Ru(O3)	0.31284(4)	0.36175(2)	0.07682(2)
O(b)	0.4537(4)	0.0594(2)	0.1925(1)
O(11)	0.4305(6)	0.1508(4)	−0.0869(2)
O(12)	0.8226(5)	0.3264(3)	0.0200(2)
O(13)	0.7184(5)	0.0495(3)	0.0998(2)
O(21)	0.0876(5)	0.2293(3)	−0.0522(2)
O(22)	0.2004(6)	−0.0257(3)	0.0503(2)
O(23)	−0.0275(4)	0.1943(3)	0.1660(2)
O(31)	0.1441(6)	0.4535(3)	−0.0492(2)
O(32)	0.0585(4)	0.4112(2)	0.1602(2)
O(33)	0.5072(6)	0.5320(3)	0.1063(2)
C(b)	0.4042(5)	0.1277(3)	0.1660(2)
C(11)	0.4673(6)	0.1763(4)	−0.0334(2)
C(12)	0.7187(6)	0.2883(4)	0.0352(3)
C(13)	0.6491(5)	0.1137(3)	0.0826(2)
C(21)	0.1502(6)	0.2204(3)	0.0014(2)
C(22)	0.2206(6)	0.0489(3)	0.0637(2)
C(23)	0.0727(5)	0.1873(3)	0.1366(2)
C(31)	0.2065(6)	0.4172(3)	−0.0035(2)
C(32)	0.1561(5)	0.3910(3)	0.1310(2)
C(33)	0.4351(6)	0.4667(3)	0.0959(2)
C(41)	0.3647(4)	0.3114(3)	0.2844(2)
C(42)	0.4659(5)	0.3796(3)	0.2657(2)
C(43)	0.6109(4)	0.3366(3)	0.2616(2)
C(44)	0.6029(4)	0.2419(3)	0.2835(2)
C(45)	0.4507(4)	0.2263(2)	0.2972(2)
C(51)	0.2050(5)	0.3257(4)	0.3044(2)
C(52)	0.4353(6)	0.4807(3)	0.2641(2)
C(53)	0.7533(5)	0.3858(3)	0.2464(2)
C(54)	0.7333(5)	0.1751(3)	0.2950(2)
C(55)	0.3871(6)	0.1428(3)	0.3277(2)
H(b)	0.6060(87)	0.2924(47)	0.1433(37)
H(13)	0.4430(69)	0.3182(39)	0.0136(30)

TABLE 3C

POSITIONAL PARAMETERS OF $(\eta^5\text{-Me}_5\text{C}_5)\text{Rh}(\mu\text{-H})_2\text{Ru}_3(\mu\text{-H})_2(\text{CO})_9$ (**4b**)

Atom	*x*	*y*	*z*
Rh	0.98037(3)	0.59288(2)	0.73039(3)
Ru(O1)	1.04956(3)	0.71566(2)	0.82189(3)
Ru(O2)	0.96976(3)	0.72580(3)	0.63514(3)
Ru(O3)	0.86620(3)	0.70897(2)	0.72228(3)
Rh′	0.43551(3)	−0.35214(2)	0.17294(3)
Ru(1′)	0.55334(3)	−0.27490(2)	0.30607(3)
Ru(2′)	0.48330(3)	−0.40632(3)	0.34438(3)
Ru(3′)	0.59610(3)	−0.41946(3)	0.26693(3)
C(11′)	0.6439(4)	−0.2278(3)	0.3999(4)
C(11)	1.0960(4)	0.8037(4)	0.8830(4)
C(12′)	0.5654(4)	−0.2287(4)	0.2140(5)
C(12)	1.0518(4)	0.6620(3)	0.9162(4)
C(13′)	0.4653(5)	−0.2121(4)	0.2993(5)
C(13)	1.1532(4)	0.6777(4)	0.8286(4)
C(21′)	0.5591(4)	−0.4460(4)	0.4522(4)
C(21)	0.9337(5)	0.8242(4)	0.6103(4)
C(22′)	0.3990(5)	−0.3731(4)	0.3824(4)
C(22)	1.0590(5)	0.7316(5)	0.5993(5)
C(23′)	0.4315(5)	−0.4973(4)	0.3025(4)
C(23)	0.8908(5)	0.6899(4)	0.5285(5)
C(31′)	0.6788(4)	−0.4593(4)	0.3708(5)
C(31)	0.8218(4)	0.8050(4)	0.6977(4)
C(32′)	0.5547(4)	−0.5107(4)	0.2198(4)
C(32)	0.7820(4)	0.6693(4)	0.6212(5)
C(33′)	0.6679(4)	−0.4075(4)	0.2083(5)
C(33)	0.8121(4)	0.6851(4)	0.7952(5)
C(41′)	0.3638(4)	−0.4008(3)	0.0452(4)
C(41)	0.9192(3)	0.4850(3)	0.7088(3)
C(42′)	0.3939(4)	−0.3303(3)	0.0369(4)
C(42)	0.9795(4)	0.4930(3)	0.7966(4)
C(43′)	0.3552(4)	−0.2783(4)	0.0703(4)
C(43)	1.0618(3)	0.5007(3)	0.7989(3)
C(44′)	0.3059(4)	−0.3169(4)	0.1043(4)
C(44)	1.0520(3)	0.5032(3)	0.7128(3)
C(45′)	0.3100(4)	−0.3921(4)	0.0867(4)
C(45)	0.9646(3)	0.4903(3)	0.6574(3)
C(51′)	0.3831(5)	−0.4690(4)	0.0103(4)
C(51)	0.8269(4)	0.4686(4)	0.6783(5)
C(52′)	0.4471(5)	−0.3141(5)	−0.0109(5)
C(52)	0.9593(5)	0.4825(4)	0.8735(4)
C(53′)	0.3595(6)	−0.1967(5)	0.0629(6)
C(53)	1.1426(4)	0.4999(4)	0.8774(4)
C(54′)	0.2498(5)	−0.2833(6)	0.1404(6)
C(54)	1.1227(4)	0.5068(4)	0.6840(4)
C(55′)	0.2615(5)	−0.4512(5)	0.1083(5)
C(55)	0.9295(4)	0.4799(4)	0.5620(4)
O(11′)	0.6968(3)	−0.1980(3)	0.4537(3)
O(11)	1.1313(3)	0.8512(3)	0.9257(4)
O(12′)	0.5759(4)	−0.2003(3)	0.1600(4)
O(12)	1.0521(4)	0.6331(3)	0.9747(3)
O(13′)	0.4132(4)	−0.1753(3)	0.2985(5)
O(13)	1.2160(3)	0.6576(3)	0.8330(4)
O(21′)	0.5994(3)	−0.4699(3)	0.5172(3)

TABLE 3C (continued)

Atom	x	y	z
O(21)	0.9135(4)	0.8825(3)	0.5952(4)
O(22′)	0.3494(4)	−0.3530(4)	0.4014(4)
O(22)	1.1112(4)	0.7348(5)	0.5773(5)
O(23′)	0.4006(4)	−0.5514(3)	0.2791(4)
O(23)	0.8452(4)	0.6673(4)	0.4634(3)
O(31′)	0.7286(3)	−0.4839(3)	0.4307(3)
O(31)	0.7925(4)	0.8615(3)	0.6846(4)
O(32′)	0.5309(4)	−0.5671(3)	0.1909(4)
O(32)	0.7317(3)	0.6441(3)	0.5614(4)
O(33′)	0.7073(4)	−0.4016(3)	0.1714(4)
O(33)	0.7772(4)	0.6693(4)	0.8354(4)
H(B2′)	0.4195(43)	−0.3598(40)	0.2651(45)
H(B2)	1.0072(44)	0.6364(41)	0.6582(44)
H(B3′)	0.5317(44)	−0.3753(41)	0.1770(45)
H(B3)	0.8994(43)	0.6254(41)	0.7576(45)
H(12′)	0.5449(43)	−0.3267(41)	0.3916(45)
H(12)	1.0414(44)	0.7597(40)	0.7311(45)
H(13′)	0.6387(43)	−0.3330(41)	0.3175(44)
H(13)	0.9460(43)	0.7521(40)	0.8098(44)

For **4b** (and **4b′**) some hydrogen atoms of the methyl groups were located on difference Fourier maps in geometrically reasonable positions. The remaining methyl hydrogen atoms were placed in calculated positions as for **3b** above. Neither their positions nor their temperature factors (assigned to be $B = 7$) were refined. All non-hydrogen atoms with the exception of C41–C45 and C41′–C45′ were allowed to refine anisotropically (527 parameters). The 8 bridging hydrogen atoms on the two independent molecules were located on difference maps and their positions (but not their temperature factors, assigned as $B = 5$) were refined. A final difference map showed no peaks higher than 0.6 eÅ^{-3}. The final discrepancy factors are given in Table 2 *. Atomic positional parameters are given in Table 3, Parts a, b, and c.

Description of the structures and discussion

Overall structure. The crystals of the three derivatives each consist of discrete molecular units whose geometries and atom numbering are given in Fig. 1, 2 and 3, respectively. We omit drawing a direct line between adjoining metal atoms on the bridged edges of the metal polyhedra because we believe that the connectivity between such metal atoms is established through the bridging atoms [12].

In **3a** and **3b** a CO group is found bridging between Rh and an Ru atom and one of the two cluster hydrogen atoms is found bridging an edge of the Ru_3 triangle. The second cluster hydrogen, however, is differently placed; in **3a** this bridges a second edge of the Ru_3 triangle, while in **3b** the second cluster hydrogen atom is found

---

* The observed and calculated structure factor amplitudes as well as Tables of Supplementary Interatomic Distances and Angles and least squares planes for the Cp or Cp* rings have been deposited with the National Auxiliary Publications Service, c/o Microfiche Publications, P.O.: Box 3513, Grand Central Station, New York, N.Y. 10017, U.S.A.

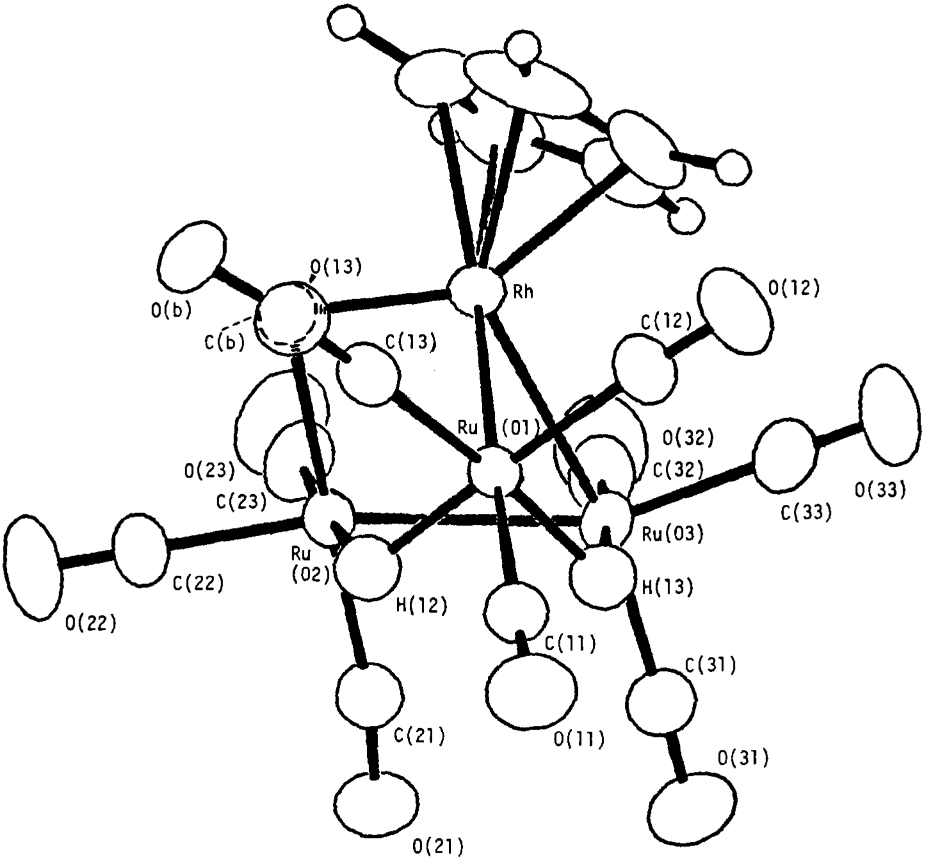

Fig. 1. ORTEP projection of **3a**, $(\eta^5\text{-}C_5H_5)Rh(\mu\text{-}CO)Ru_3(\mu\text{-}H)_2(CO)_9$; thermal ellipsoids or spheres (for H atoms) at 50% probability. H atoms of $(\eta\text{-}C_5H_5)$ ring not refined.

bridging another Rh–Ru edge of the metal polyhedron. These structures parallel the isomers found in the Co/Os_3 homologues, namely, $(\eta\text{-}C_5H_5)Co(\mu\text{-}CO)Os_3(\mu\text{-}H)_2(CO)_9$ (**6a**), [3b], and $(\eta\text{-}C_5Me_4Et)Co(\mu\text{-}CO,\mu\text{-}H)Os_3(\mu\text{-}H)(CO)_9$ (**6b**) [4]. There are similar parallels in the disposition of the bridging CO group with respect to the metal polyhedron, see next section.

In **4b** the four cluster hydrogen atoms are found bridging four separate edges of the metal polyhedron, two between Rh and Ru atoms and the other two between two Ru atoms.

Comparison of selected interatomic distances. Selected data are presented in Table 4; remaining interatomic distances are deposited together with the structure factor tables, see footnote immediately preceding. Unbridged M–M′ fall in the range 2.70–2.81 Å, regardless whether M = M′ = Ru or M = Ru or M′ = Rh. The same is true for hydrogen bridged M–(H)–M′ distances which fall in the range 2.87–2.91 Å, respectively.

These separations are similar to what is observed in $Ru_2Rh_2(\mu\text{-}H)_2(CO)_{12}$ (**8**) [2]. Metals bridged by CO, on the other hand, are separated by distances quite close to those for unbridged M–M separations. Similar or very slightly shorter values are

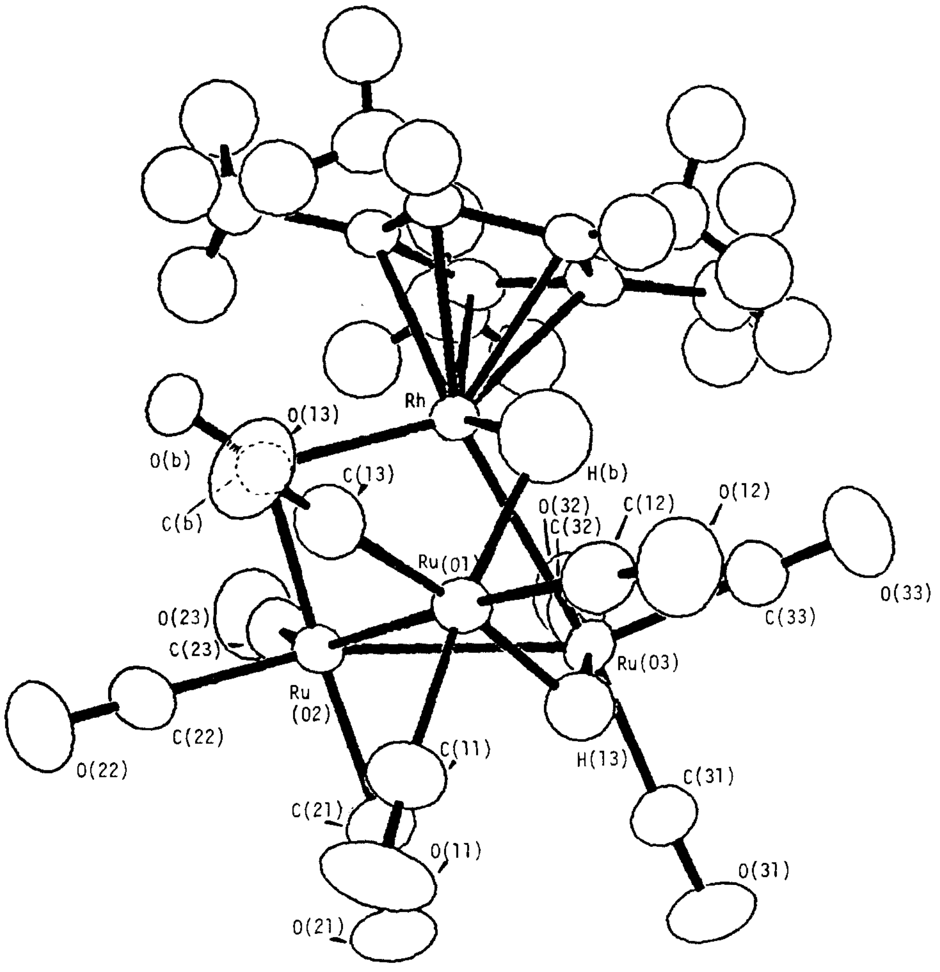

Fig. 2. ORTEP projection of **3b**, $(\eta^5\text{-}Me_5C_5)Rh(\mu\text{-}CO,\mu\text{-}H)Ru_3(\mu\text{-}H)(CO)_9$; thermal ellipsoids or spheres (for H atoms) at 50% probability. H atoms of $(\eta\text{-}C_5Me_5)$ ring not refined.

observed in the Co/Os_3 cluster complexes **6a** and **6b** [3b,4], respectively.

Separations of M to C(b) (carbon atom of the bridging CO) are also presented in Table 4. The asymmetry seen in **3a** is paralleled in **6a** [4], (C(b) = C(41)), Å: Co–C(41), 1.789(14); Os(1)–C(41), 2.208(13), while the more nearly equal M–C(b) separations in **3b** are seen in **6b** [3b] (making allowance for the difference in atomic radii for the latter two metals), (C(b) = C(12)), Å: Co(1)–C(12), 1.918(11); Os(1)–C(12), 2.071(11).

Selected interatomic angles. These are presented in Table 5, parts a through e. We have grouped the angles to reflect the coordination around the metal atoms. For each of the three Ru atoms, we trace the angles from the carbon atoms of each of the attached three CO groups to atoms placed either *pseudo-trans* or *pseudo-cis* in the coordination sphere around the metals, Table 5. Parts a, b, c. *Pseudo*-octahedral coordination is especially evident around atoms Ru(O1) in each of the three Figures. Bridging hydrogen atoms appear closest to ideal octahedral positions relative to the

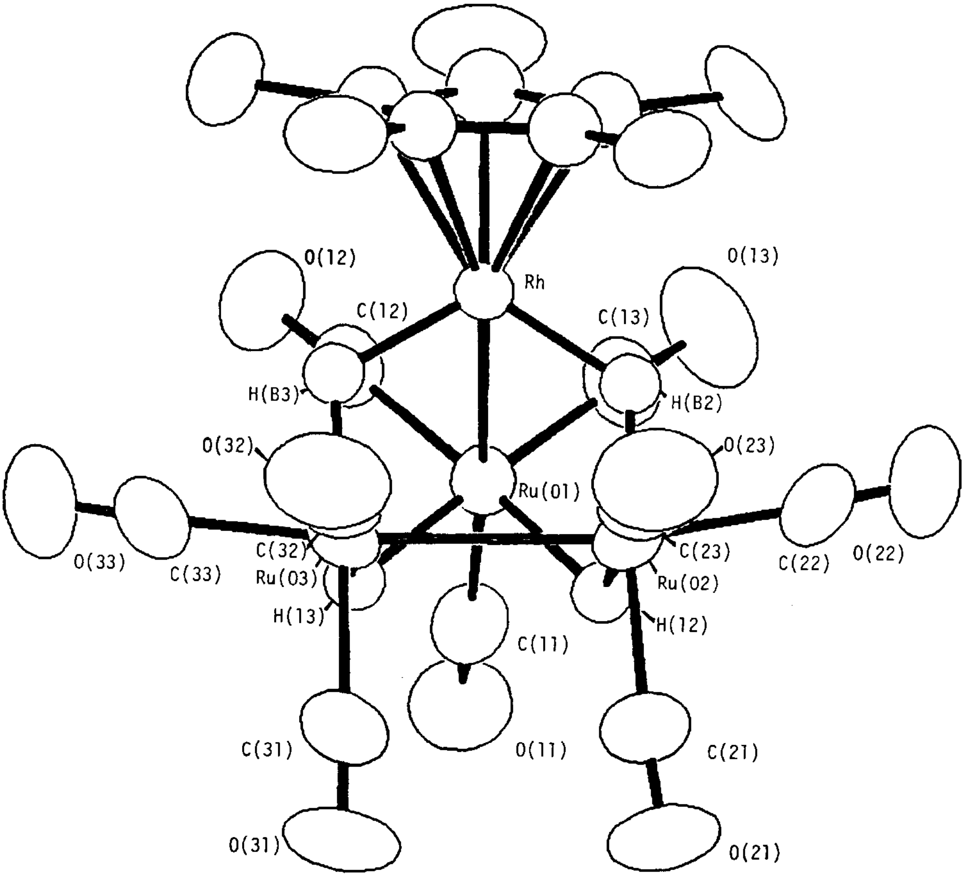

Fig. 3. ORTEP projection of **4b**, $(\eta^5\text{-Me}_5C_5)Rh(\mu\text{-H})_2Ru_3(\mu\text{-H})_2(CO)_9$; thermal ellipsoids or spheres (for H atoms) at 50% probability. H atoms of $(\eta\text{-C}_5Me_5)$ ring omitted for clarity.

carbonyl groups, i.e. in the range 170–177° for *trans* dispositions and in the range 77–89° for *cis* dispositions. Other angles deviate more extensively from the ideal octahedral values owing to the geometry imposed by the metal framework.

The angles between metal atoms within the metal polyhedra fall in the range 56–64° (Supplemental Table S 4, Parts a, b, and c) which is observed in other like structures (**3b**,**4**). A few inter-metal angles are to be found in the data displayed in Table 5 (parts c and d).

Parallels between **3a** and **6a** are also found in the bond angles around C(b), the bridging carbonyl group (Supplementary Table S4). In **3a** (deg): Rh–C(b)–O(b), 144; Ru(O2)–C(b)–O(b), 134, and, Ru(O2)–C(b)–Rh, 82. In **6a**, the corresponding values are (deg): Co–C(41)–O(41), 146; Os(1)–C(41)–O(41), 132, and, Os(1)–C(41)–Co, 82 (**3b**). By comparison, in **3b** the corresponding values are (deg): Rh–C(b)–O(b), 132; Ru(O2)–C(b)–O(b), 143, and Ru(O2)–C(b)–Rh, 84.

To describe the disposition of the cyclopentadienyl rings with respect to the metal polyhedra, least squares planes were calculated from the positions of the ring carbon atoms for each Cp or Cp* group. The angle (β) could then be defined and compared, see Table 5, part e and footnote. In the structures containing a bridging

TABLE 4

COMPARISON OF SELECTED INTERATOMIC SEPARATIONS (Å) [a]

Type of separation:	Ru(*n*)–Ru(*m*)					
	n–*m*	**3a**	*n*–*m*	**3b**	*n*–*m*	**4b & 4b′**
Ru–Ru	2–3	2.765(1)	1–2	2.8086(4)	2–3	2.809(1)
			2–3	2.7679(4)	2′–3′	2.813(1)
Ru–μ(H)–Ru	1–2	2.938(1)	1–3	2.8969(4)	1–2	2.926(1)
	1–3	2.870(1)			1′–2′	2.912(1)
					1–3	2.938(1)
					1′–3′	2.924(1)
	Rh–Ru(*m*)					
Rh–Ru	Rh–1	2.723(1)	Rh–3	2.7386(4)	Rh–1	2.735(1)
	Rh–3	2.707(1)			Rh′–1′	2.752(1)
Rh–μ-(CO)–Ru	Rh–2	2.727(1)	Rh–2	2.7515(4)		
					Rh–2	2.912(1)
Rh–μ-(H)–Ru			Rh–1	2.9169(4)	Rh′–2′	2.888(1)
					Rh–3	2.891(1)
					Rh′–3′	2.871(1)

Ru(*n*)–H(*m*) or Rh–H(*m*)							
3a		**3b**		**4b & 4b′**			
1–12	1.69(6)	1–13	1.76(6)	1–12	1.71(7)	2–B2	1.76(8)
1–13	1.68(8)	3–13	1.91(6)	1′–12′	1.81(7)	2′–B2′	1.60(7)
2–12	1.92(6)	1–B	2.04(7)	2–12	1.71(7)	Rh–B2	1.70(7)
3–13	1.94(7)	Rh–B	1.80(8)	2′–12′	1.80(7)	Rh′–B2′	1.72(7)
				1–13	1.86(7)	3–B3	1.76(7)
				1′–13′	1.78(7)	3′–B3′	1.69(7)
				3–13	1.67(7)	Rh–B3	1.77(7)
				3′–13′	1.82(7)	Rh′–B3′	1.71(7)

	Rh–C(*b*)	Ru(2)–C(*b*)	C(b)–O(*b*)
3a	1.924(5)	2.220(5)	1.157(7)
3b	2.054(4)	2.049(4)	1.180(5)

	Rh–C(*m*) of C_5 ring)			
	3a	**3b**	**4b**	**4b′**
Rh–C(41)	2.255(7)	2.243(3)	2.216(6)	2.214(6)
Rh–C(42)	2.251(6)	2.278(3)	2.170(6)	2.178(6)
Rh–C(43)	2.200(6)	2.194(3)	2.215(6)	2.206(7)
Rh–C(44)	2.219(6)	2.224(3)	2.171(5)	2.170(6)
Rh–C(45)	2.217(6)	2.241(3)	2.224(6)	2.199(6)

[a] E.s.d. of the last digit given in parentheses.

CO group (**3a** or **3b**), the Cp or Cp* ring is tilted away from this group, with a significantly larger angle with respect to the Ru_3 plane than in **4b**; this is paralleled by a similar angle of 163° in **6b** [4].

Placement of the bridging atoms relative to the metal polyhedra. Selected data are given in Table 6. Hydrogen atoms bridging the Ru_3 triangle are similarly placed

TABLE 5

SELECTED INTERATOMIC ANGLES

Part a. Interatomic angles around Ru(1) [a]

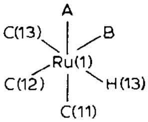

	3a, 4b	3b
A	Rh	H(B)
B	H(12)	Ru(2)

	"*trans*" angles (deg)			
	3a	**3b**	**4b**	**4b′**
C(11)-Ru(1)-A	173.7(2)	172.(2)	178.2(2)	174.4(2)
C(12)-Ru(1)-B	177.(2)	164.6(2)	175.(2)	175.(2)
C(13)-Ru(1)-H(13)	171.(2)	169.(2)	177.(2)	177.(2)
	"*cis*" angles (deg)			
C(11)-Ru(1)-H(13)	77.(2)	77.(2)	86.(2)	80.(2)
C(11)-Ru(1)-C(12)	95.4(2)	99.9(2)	97.0(3)	99.1(3)
C(11)-Ru(1)-C(13)	94.4(2)	93.2(2)	96.0(3)	97.9(3)
C(11)-Ru(1)-B	84.(2)	86.0(2)	87.(2)	83.(2)
C(12)-Ru(1)-H13	89.(3)	83.(2)	87.(2)	89.(2)
C(12)-Ru(1)-C(13)	93.5(2)	94.3(2)	94.4(3)	92.6(3)
C(12)-Ru(1)-A	86.2(2)	77.(2)	84.6(2)	80.9(2)
C(13)-Ru(1)-A	91.6(2)	95.(2)	84.8(2)	87.7(2)
C(13)-Ru(1)-B	89.(2)	99.7(1)	87.(2)	92.(2)
H(13)-Ru(1)-A	97.(2)	95.(3)	93.(2)	95.(2)
H(13)-Ru(1)-B	88.(2)	85.(2)	91.(3)	87.(3)
A-Ru(1)-B	94.(2)	95.(2)	91.(2)	97.(2)

[a] E.s.d. of last digit cited is given in parentheses.

Part b. Interatomic angles around Ru(2) [a]

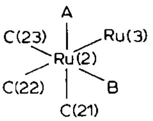

	3a	3b	4b
A	C(b)	C(b)	H(B2)
B	H(12)	Ru(1)	H(12)

	"*trans*" angles (deg)			
	3a	**3b**	**4b**	**4b′**
C(21)-Ru(2)-A	176.2(2)	173.5(2)	178.(2)	169.(3)
C(22)-Ru(2)-Ru(3)	166.6(2)	159.3(1)	167.6(2)	165.0(2)
C(23)-Ru(2)-B	177.(2)	155.8(1)	179.(2)	172.(2)
	"*cis*" angles (deg)			
C(21)-Ru(2)-C(22)	96.1(3)	93.7(2)	96.5(3)	96.3(3)
C(21)-Ru(2)-C(23)	93.1(3)	97.6(2)	94.4(3)	93.2(3)
C(21)-Ru(2)-Ru(3)	75.8(1)	71.1(1)	89.9(2)	95.0(2)
C(21)-Ru(2)-B	88.(2)	90.9(1)	85.(2)	80.(2)
C(22)-Ru(2)-C(23)	95.9(3)	97.2(2)	94.0(3)	95.6(3)
C(22)-Ru(2)-A	84.6(2)	84.4(2)	81.(2)	76.(2)
C(22)-Ru(2)-B	87.(2)	104.9(2)	86.(2)	89.(2)
C(23)-Ru(2)-A	90.6(2)	98.9(2)	87.(2)	96.(3)
C(23)-Ru(2)-Ru(3)	95.2(2)	98.7(1)	96.1(2)	93.5(2)
Ru(3)-Ru(2)-A	102.8(1)	106.1(1)	92.(2)	91.(2)
Ru(3)-Ru(2)-B	83.(2)	62.6(1)	84.(2)	83.(2)
A-Ru(2)-B	88.(2)	73.9(1)	94.(2)	91.(3)

[a] E.s.d. of last digit cited is given in parentheses.

TABLE 5

SELECTED INTERATOMIC ANGLES

Part c. Interatomic Angles around Ru(3) [a]

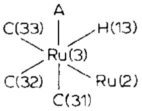

	3a, 3b	4b
A	Rh	H(B3)

	"*trans*" angles (deg)			
	3a	**3b**	**4b**	**4b′**
C(31)–Ru(3)–A	167.0(2)	173.3(1)	170.(2)	173.(2)
C(32)–Ru(3)–H(13)	176.(2)	170.(2)	174.(2)	177.(2)
C(33)–Ru(3)–Ru(2)	155.8(2)	153.4(2)	169.0(2)	168.0(2)
	"*cis*" angles (deg)			
C(31)–Ru(3)–C(32)	95.9(3)	93.9(2)	93.9(3)	93.7(3)
C(31)–Ru(3)–C(33)	94.8(3)	91.5(2)	95.3(3)	97.5(3)
C(31)–Ru(3)–H(13)	83.(2)	82.(2)	83.(2)	84.(2)
C(31)–Ru(3)–Ru(2)	107.9(2)	113.4(1)	94.1(2)	89.8(2)
C(32)–Ru(3)–C(33)	93.6(3)	98.0(2)	96.1(3)	95.5(3)
C(32)–Ru(3)–A	89.1(2)	85.7(1)	90.(2)	93.(2)
C(32)–Ru(3)–Ru(2)	92.4(2)	89.9(1)	88.8(2)	93.6(2)
C(33)–Ru(3)–A	96.8(2)	95.2(1)	75.(2)	78.(2)
C(33)–Ru(3)–H(13)	90.(2)	92.(2)	89.(2)	86.(2)
H(13)–Ru(3)–Ru(2)	85.(2)	83.(2)	87.(2)	86.(2)
H(13)–Ru(3)–A	92.(2)	97.(2)	94.(3)	90.(3)
Ru(2)–Ru(3)–A	59.77(1)	59.95(1)	95.(2)	94.(2)

[a] E.s.d. of last digit cited is given in parentheses.

Part d. Interatomic "cis" angles around Rh(deg) [a]

3a		**3b**	
Ru(1)–Rh–C(b)	80.9(2)	H(b)–Rh–C(b)	104.(2)
Ru(3)–Rh–C(b)	114.1(2)	Ru(3)–Rh–C(b)	107.0(1)
Ru(1)–Rh–Ru(3)	65.24(1)	Ru(3)–Rh–H(b)	77.(2)

	4b	**4b′**
Ru(1)–Rh–H(B2)	81.(2)	68.(2)
H(B3)–Rh–H(B2)	122.(3)	118.(3)
H(B3)–Rh–Ru(1)	77.(2)	73.(2)

[a] E.s.d. of last digit cited is given in parentheses; angles from C(η-C_5H_5) to Rh in **3a** or from C(η-C_5Me_5) to Rh in **3b** or **4b** are given in the Supplemental Data.

Part e. Disposition of cyclopentadienyl ring, β (deg) [a]

3a:	158	**3b**:	166	**4b**:	173	**4b′**	177

[a] β is the external angle between the normal from Rh to the least-squares plane of 5 carbon atoms in the Cp ring to the normal from Rh to the Ru_3 plane. Data for least-squares planes have been deposited with the Supplementary Materials.

TABLE 6

PLACEMENT OF BRIDGING ATOMS RELATIVE TO THE METAL POLYHEDRA

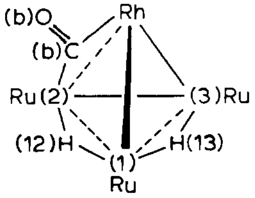

(3a)

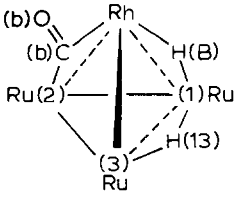

(3b)

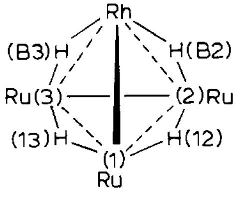

(4b)

Planes	Angle (deg) [a]		Separation (Å) [b]
	3a		
A. Ru(1)–H(12)–Ru(2)	A to B	127.0	H(12) to B 0.837
B. Ru(1)–Ru(2)–Ru(3)	C to B	125.4	H(13) to B 0.888
C. Ru(1)–H(13)–Ru(3)			
D. Rh–C(b)–Ru(2)	D to E	169.5	C(b) to E 0.2
E. Rh–Ru(2)–Ru(3)			
	3b		
F. Ru(1)–H(13)–Ru(3)	F to G	127.0	H(13) to G 0.917
G. Ru(1)–Ru(2)–Ru(3)			
H. Rh–H(14)–Ru(1)	H to I	171.6	H(14) to I 0.181
I. Rh–Ru(1)–Ru(2)	J to I	87.9	C(b) to I 1.521
J. Rh–C(b)–Ru(2)			
	4b and **4b′**		
K. Rh–H(B2)–Ru(2)	K to L	168.2	H(B2) to L 0.2
L. Rh–Ru(2)–Ru(3)	K′ to L′	168.8	H(B2)′ to L′ 0.2
M. Rh–H(B3)–Ru(3)	M to L	176.6	H(B3) to M 0.06
	M′ to L′	175.1	H(B3)′ to M′ 0.08
P. Ru(1)–H(12)–Ru(2)	P to Q	131.8	H(12) to Q 0.7
Q. Ru(1)–Ru(2)–Ru(3)	P′ to Q′	120.5	H(12)′ to Q′ 0.9
R. Ru(1)–H(13)–Ru(3)	R to Q	109.7	H(13) to Q 0.8
	R′ to Q′	129.6	H(13)′ to Q′ 0.08

[a] Exterior angle (supplement of the angle between normals to the planes) e.s.d. ca. 1.0°. [b] E.s.d. ca. 0.1 Å.

"below" the Ru_3 plane (i.e. "away" from the Rh atom) with "exterior" interplanar angles (Ru–H–Ru′)–(Ru_3) in the range 110–130°. By comparison, similar placement is found for the hydrogen atoms bridging edges of the Os_3 triangle with respect to the Os_3 plane in **6a**; the corresponding interplanar angles are, for H(12), 125° and for H(23) 146° [3b].

Conclusion

The complexes studied here are synthesized easily enough by displacing CO with a stream of H_2 gas from suitable starting materials at slightly elevated temperatures. These clusters, however, are easily disrupted back into the starting materials under CO atmosphere at very mild conditions (and complete exchange under ^{13}CO). By comparison with homologous Co/Os_3 clusters, we find it most interesting that despite some differences in the required conditions for the disruption reactions accompanied by complete exchange in the metal atoms of the clusters, subtle structural differences between homologous unsubstituted and substituted cyclopentadienyl derivatives in the two series of complexes are maintained.

Acknowledgment

We thank the Royal Society (London) for a Fellowship, and the Council for International Exchange of Scholars for a Fulbright Scholarship (both to W.E.L. for a period of residence at U.C.L.A.), the National Science Foundation (U.S., Grant CHE-81-11332, to HDK) for support and Dr. Dilip Sensharma at UCLA for expert assistance with the FAB-MS.

References

1 M.J. Mays, P.R. Raithby, P.L. Taylor and K. Henrick, J. Organomet. Chem., 224 (1982) C45.

2 J. Pursiainen and T.A. Pakkanen, J. Chem. Soc., Chem. Commun., (1984) 252.

3 (a) J.S. Plotkin, D.G. Alway, C.R. Weisenberger and S.G. Shore, J. Am. Chem. Soc., 102 (1980) 6156; (b) M.R. Churchill, C. Bueno, S. Kennedy, J.S. Bricker, J.S. Plotkin and S.G. Shore, Inorg. Chem., 21 (1982) 627; (c) L.-Y. Hsu, W.-L. Hsu, D.-Y. Jan, A.G. Marshall and S.G. Shore, Organometallics, 3 (1984) 591.

4 J. Lewis, R.B.A. Pardy and P.R. Raithby, J. Chem. Soc. Dalton Trans., (1982) 1509.

5 W.E. Lindsell, C.B. Knobler and H.D. Kaesz, J. Chem. Soc. Chem. Commun., (1985) in press.

6 (a) P.T. Barger and J.E. Bercaw, J. Organomet. Chem., 201 (1980) C39; (b) idem., Organometallics, 3 (1984) 278; (c) R. Colton and C.J. Commons, Aust. J. Chem., 28 (1975) 1673; (d) C.J. Commons and B.F. Hoskins, ibid., 1663.

7 J.R. Fox, W.L. Gladfelter and G.L. Geoffroy, Inorg. Chem., 19 (1980) 2574.

8 J.F. Knifton, J. Chem. Soc. Chem. Commun., (1983) 729.

9 (a) M.I. Bruce, J.G. Matisons, R.G. Wallis, J.M. Patrick, B.W. Skelton, and A.H. White, J. Chem. Soc. Dalton Trans., (1983) 2365; (b) C.M. Jensen and N.L. Jones, Inorganic Syntheses XXV, in preparation; (c) E.O. Fischer and K. Bittler, Z. Naturforsch. B, 16 (1961) 225.

10 (a) S.A.R. Knox, J.W. Koepke, M.A. Andrews and H.D. Kaesz, J. Am. Chem. Soc., 97 (1975) 3942; (b) R. Hill and S.A.R. Knox, J. Chem. Soc. Dalton Trans., (1975) 2622; (c) R.J. Lawson and J.R. Shapley, J. Am. Chem. Soc., 98 (1976) 7433.

11 (a) International Tables for X-Ray Crystallography, Vol. IV, Kynoch Press, Birmingham, 1975; (b) R.F. Stewart, E.R. Davidson and W.T. Simpson, J. Chem. Phys., 42 (1965) 3175.

12 (a) R. Mason and D.M.P. Mingos, J. Organomet. Chem., 50 (1973) 53; (b) B.K. Teo, M.B. Hall, R.F. Fenske and L.F. Dahl, ibid., 70 (1974) 413; (c) M. Berry, N.J. Cooper, M.L.H. Green and S.J. Simpson, J. Chem. Soc. Dalton Trans., (1980) 37; (d) E.D. Jemmis, A.R. Pinhas and R. Hoffmann, J. Am. Chem. Soc., 102 (1980) 2576; (e) N.M. Kostic and R.F. Fenske, Inorg. Chem., 22 (1983) 666.

Note added in proof. The reaction of **5** with CO leads to a mixture of $Cp^{*}Rh(CO)_2$, $Ru(CO)_5$ and $Ru_3(CO)_{12}$ in ca. 22 h ($t_{1/2}$ ca. 4 h) going through an intermediate associated with bands 2086, 2049 and 1965 cm^{-1}.

For recent reports of other Ru/Rh mixed metal cluster complexes, see L.J. Farrugia, J.C. Jeffery, C. Marsden and F.G.A. Stone, J. Chem. Soc., Dalton Trans., (1985) 645, and R.P. Hughes, A.L. Rheingold, W.A. Herrmann and J.L. Hubbard, J. Organomet. Chem., 286 (1985) 361.